AN AIR-ASSISTED FLARE FOR BIOMASS GASIFIERS

Hayder A. Alhameedi, Aso A. Hassan, Joseph D. Smith, Ph.D.
Missouri University of Science and Technology, Rolla, Missouri, USA

Robert E. Jackson and Zachary P. Smith
Elevated Analytics Consulting, Inc., Provo, Utah, USA

ABSTRACT

Computational fluid dynamics (CFD) was used to simulate the combustion practice of the gases that produce from gasification process. In this simulation a new air-assisted flare design which capable to handle low flowrates of these gases with high performance was used. The simulated cases were performed by using the gases that produced in the downdraft gasifier at our lab. Wood pellet was used as the biomass feedstock of the gasification process in the current study which results mainly CO, H2, CH4, and CO2 as gasification gases. Different low flowrates of these gases were used in the simulation. The non-premixed Steady Diffusion flamelet combustion model was used in this study with 22-species reduced reaction mechanism to predict the combustion efficiency of gasification gases. The results show a good flare performance when the new flare design is used.

INTRODUCTION

Gasification of biomass to produce bio syngas has received increased attention in recent years due to an increased demand for renewable energy. Also, for some regions biomass gasification is the most economical way to produce syngas due to the large amounts of biomass available and the respective lack of fuel gas to fire steam boiler [1] [2]. The produced gases from the biomass gasification process mainly include carbon monoxide, hydrogen, carbon dioxide, methane, and water. The syngas components depend on several factors including feedstock composition, feedstock shape, equivalence ratio in the gasifier, reactor temperature and pressure, and the type of gasifier used. Several different types of gasifiers have been developed and are used including updraft and downdraft fixed bed gasifiers, moving bed gasifiers, fluidized bed gasifiers, and entrained flow gasifiers.

In a Downdraft Fixed Bed Gasifier (DFBG) there are four main zones in the reactor; 1) drying zone, 2) pyrolysis zone, 3) combustion zone, and 4) reduction zone. Different exothermic and endothermic reactions take place within these regions to produce the bio syngas. An advantage of a DFBG over an updraft fixed bed gasifier is that the syngas contains less tar because it exits the gasifier from the hottest zone at the bottom [3]. Also, more attention is taken by researchers on DFBG because of its possibility to produce local energy at a reasonable cost [4].

Flares are often used with these gasifiers to ensure personnel safety in the plant by burning noxious gases during startup and shutdown of the gasifier. In general, flares are designed to work best at maximum capacity during a plant upset condition which helps avoid catastrophic damage in the equipment. During the startup/shutdown conditions, flares often must operate at low flow conditions which reduces flare performance. Two parameters are routinely used to quantify flare performance including combustion efficiency (CE) and destruction removal efficiency (DRE).

Many experimental and simulation studies have been conducted on the combustion of bio syngas in various combustion equipment. Zhou et al. studied the effect of syngas composition and the initial pressure on the laminar flame speed [5]. Kai Zhang and Xi Jiang investigated the influence of syngas composition on combustion efficiency using uncertainty quantification [6]. However, very few studies have considered syngas combustion characteristics in gas flares.

Several studies have also been performed to quantify the effect of operating parameters on flare performance [7] [8] [9] [10] [11] [12]. Among these studies, several researchers [7] [10] [11] have studied the impact of low flow conditions and low heating value of flare gas on flare performance. They found that low flare gas flow rate reduced flare performance. Later, Singh et al. [8] performed a numerical simulation of the same system using different combustion models [10] [11]. They showed that low flow rates resulted in lower combustion efficiency. These studies were conducted using a mixture of natural gas, propylene, with nitrogen or natural gas and nitrogen. However, these studies did not identify a way to avoid reduced flare performance at low flow rates. Also, these studies did not consider bio syngas as the flare gas.

The main objective of this work has been to use computational fluid dynamics (CFD) to study the performance of an air-assisted flare designed to handle low flow conditions of bio syngas.

FLARE PERFORMANCE PARAMETERS

The quantification of flare performance can be conducted by using two common parameters, CE and DRE. The CE is defined as the percentage of amount of fuel that converted to CO2 to the total amount of fuel that used in flaring. While the DRE is defined as the percentage of the total amount of fuel that converted to another products to the actual amount of fuel used in the flaring. The CE and DRE can be written as:

$$CE\ \% = \frac{total\ amount\ of\ CO2\ in\ flue\ gases - amount\ of\ CO2\ in\ fuel}{total\ amount\ of\ (CO+CH4+C2H6)\ in\ fuel}\ 100\ \% \quad (1)$$

$$DRE\ \% = \frac{total\ amount\ of\ (CO+CH4+C2H6)\ in\ flue\ gases}{total\ amount\ of\ (CO+CH4+C2H6)\ in\ fuel}\ 100\% \quad (2)$$

PREVIOUS STUDIES OF DOWN-DRAFT FIXED BED GASIFIERS

Several studies have been performed in the Bio Energy System Technology (BEST) lab at Missouri University of Science and Technology aimed at understanding the effect of several operating parameters on biomass gasification [13] [14] [15] [16]. Golpour et al. [14] [13] tested a DFBG and performed several experimental and theoretical studies on the overall gasification process. Table 1 shows experimental results from this work. Wood pellets were used as the biomass feedstock to produce a bio syngas which was approximately 40% by volume of the total produced gases. Measured syngas flowrates from the gasifier during this work represent a low flow condition.

Table 1. Conditions of the produced gas from DFBG [11].

	Actual gases concentration, volume fraction								
Case	**H2**	**CO**	**CO2**	**CH4**	**C2+ hydrocarbon**	**N2**	**Heating value MJ/kg**	**Temperature (ºC)**	**Flowrate ft/s**
1	18	21	16	2	2	41	28.8	35	1
2	18	21	16	2	2	41	28.8	35	2
3	18	21	16	2	2	41	28.8	35	3

COMBUSTION REACTION MECHANISM FOR BIO SYNGAS

The syngas composition affects the combustion process by changing the flame characteristics [5]. Several reaction mechanisms have been proposed and tested to simulate the combustion of the syngas [17] [5] [18] [19]. Some of these mechanisms are summarized in Table 2. Among these mechanisms, Abou-Taouuk [17] developed and evaluated a four steps reaction mechanism for syngas. This mechanism included 5 species to combust a mixture of syngas of 10% CH4, 22.5 CO and 67.5 % H2 which is shown in table. A reduced mechanism [18] was developed from Gas Research Institute (GRI) mechanism [19]. The reduced mechanism included 22 species with 104 reactions as shown in Table 2. In the current study the reduced mechanism of 22 species was selected to solve the combustion kinetics of syngas because it has lower number of both reactions and species than GRI mechanism and it has been tested against the GRI mechanism. Moreover, it has all important species in the combustion of syngas.

Table 2. Reaction mechanisms for syngas combustion.

Mechanism	Number of reactions	Number of species	Species
GRI mechanism	325	53	H_2, H, O, O_2, OH, H_2O, HO_2, H_2O_2, C, CH, CH_2, $CH_2(S)$, CH_3, CH_4, CO, CO_2, HCO, CH_2O, CH_2OH, CH_3, CH_3OH, C_2H, C_2H_2,C_2H_3,C_2H_4, C_2H_5, C_2H_6, HCCO, CH_2CO, HCCOH, N, NH, NH_2, NH_3, NNH, NO, NO_2, N_2O, HNO, CN, HCN, H_2CN, HCNN, HCNO, HOCN, HNCO, NCO, N_2, AR, C_3H_7, C_3H_8, CH_2CHO, CH_3CHO
Reduced mechanism	104	22	H_2, H, O, O_2, OH, H_2O, HO_2, H_2O_2, CH_2, $CH_2(S)$, CH_3, CH_4, CO, CO_2, HCO, CH_2O, CH_3O, C_2H_2, C_2H_3, C_2H_4, C_2H_5, C_2H_6, N_2, AR
Reduced 4-reactions mechanism	4	5	CH_4, O_2, CO, H_2, H_2O,

ANALYSIS METHODOLOGY

The CFD tool, Ansys Fluent 18.1 was used to conduct all simulation cases. A pressure-based solver with coupled algorithm was used in current CFD code. For spatial discretization, the least squared cell based was used for gradient, and second order for pressure. The second order upwind differencing scheme was used for spatial discretization of the momentum, energy, mean mixture fraction, and mixture fraction variance terms. The spatial discretization of the turbulent kinetic energy, and turbulent dissipation rate terms was used. To accelerate the CFD computations, pseudo transient method was used. For the sake of simplicity, the steady state results of CFD simulation were obtained. In order to capture the turbulence fluctuation, the k-e realizable model was used. Also, the radiation effects were neglected to reduce the computations time.

Domain and Boundary conditions

Three dimensional CFD syngas combustion was conducted using the new flare tip design. The rectangular CFD domain utilized in this study is presented in

Figure 1. The dimensions of the domain were a 100 inches in for both width and length and 150 inches in height. A 6 inch diameter and 40 inch height flare was located in the center of this domain. The assisted air was injected radially into the cross flow of the syngas from slot jet around the flare tip.

Different boundary conditions were employed in current simulations. For the inlet face of the flare, uniform velocity inlets for the syngas inlet of 1, 2, and 3ft/s were utilized. The inlet

temperature for syngas inlet was 35°C. The volumetric flowrate at the injection air was 7.4 ft^3/min Also, uniform velocity and the temperature inlet of value 25°C were used for the injected air. An atmospheric pressure outlet condition was employed at the domain outlet with pressure value of 10^{-5} pa. For the bottom face of the domain and the flare walls, the non-slip boundary condition was used. For these walls, the adiabatic wall condition was used. The effect of the gravitational force on the flow was considered. The syngas composition gases used in this study were 0.2 H_2, 0.4 CO, 0.01 CH_4, 0.15 CO_2, 0.23 H_2O, and 0.01 N_2.

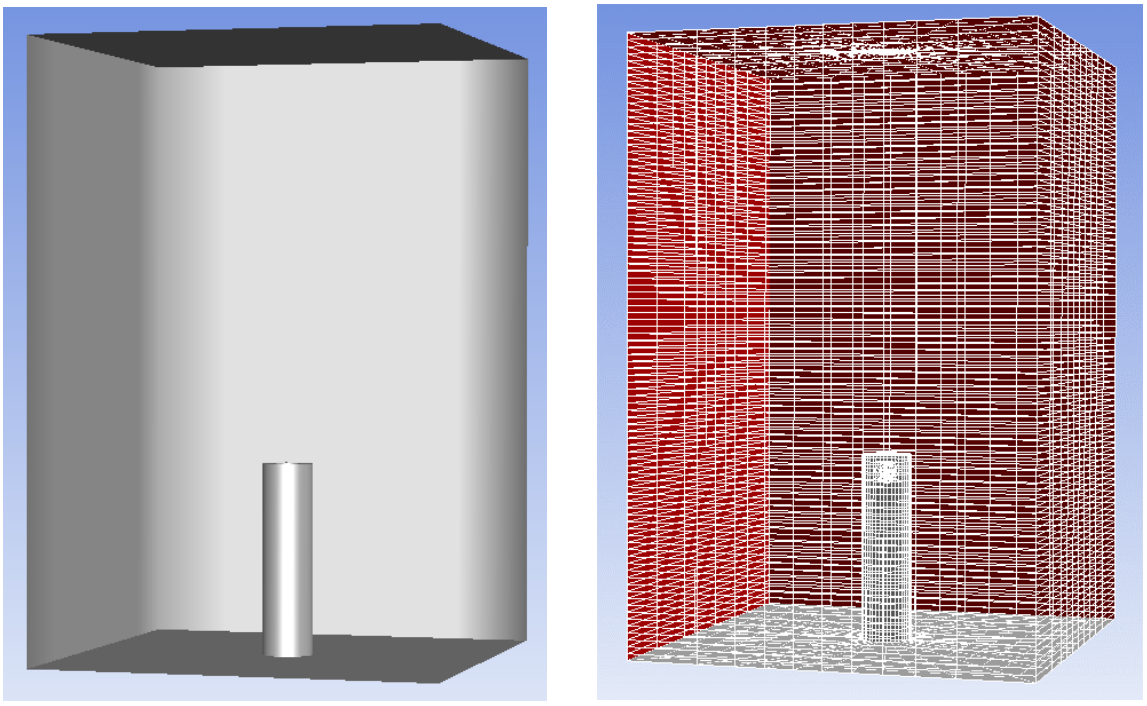

Figure 1 – System domain and computational mesh

CFD Model Basis

The combustion efficiency and destruction removal efficiency of the new flare design operating under low flow rates conditions can be predicted by using Ansys, Fluent 18.1 CFD tool. This tool is discretize the governing equations related to combustion process and solve them by using finite volume method. The steady state governing equations for the combustion process, assuming incompressible fluid flow, are given below [9] [20]:

The continuity equation is:

$$\partial(\rho u_i)/\partial x_j = 0 \tag{3}$$

with ρ as the mxiture gas density, and u_i as the ensemble-average component velocity, given by:

$$u_i = \bar{u}_i + u' \quad (4)$$

Here $\bar{u}_i$ is the mean velocity and u' is the fluctuation velocity. Based on this, the ensemble averaged momentum equation is:

$$\partial(\rho u_i u_j)/\partial x_j = -\partial P/\partial x_j + \frac{\partial}{\partial x_j}\left[\left(\mu\,(u_i + u_j - \delta_{ij}\,\frac{2}{3}\,u_k\right) - \rho\,\overline{u_i u_j}\right] \quad (5)$$

where P is the pressure, and μ is the gas mixture viscosity, and δ_{ij} is the kronecker delta function.

Reynolds stresses $\rho\,\overline{u_i u_j}$ are expressed as a function of velocity gradients using Boussinesq hypothesis as implemented in in the *k-ε* turbulence model written as:

$$\rho\,\overline{u_i u_j} = \mu_t\left(\partial u_i/\partial x_j + \partial u_j/\partial x_i\right) - \frac{2}{3}(\rho\,k - \mu_t\ \partial u_k/\partial x_k)\,\delta_{ij} \quad (6)$$

where $\mu_t$is the turbulent viscosity and k is the turbulence kinetic energy. For this model, the turbulent viscosity is calculated from the equation:

$$\mu_t = \frac{\rho\,C_\mu k^2}{\epsilon} \quad (7)$$

where k is the turbulence kinetic energy and ϵ is the turbulence dissipation rate. For the non-liner Realizable k-ϵ turbulence model, two other transport equations are required as shown in Equation 8 and 9:

$$\frac{\partial}{\partial t}(\rho k) + \frac{\partial}{\partial x_j}(\rho k u_j) = \frac{\partial}{\partial x_j}\left[\left(\mu + \frac{\mu_t}{\sigma_k}\right)\frac{\partial k}{\partial x_j}\right] + G_k + G_b - \rho\epsilon - Y_M + S_k \quad (8)$$

$$\frac{\partial}{\partial t}(\rho\varepsilon) + \frac{\partial}{\partial x_j}(\rho\varepsilon u_j) = \frac{\partial}{\partial x_j}\left[\left(\mu + \frac{\mu_t}{\sigma_\varepsilon}\right)\frac{\partial \varepsilon}{\partial x_j}\right] + \rho C_1 S_\varepsilon - \rho C_2 \frac{\varepsilon^2}{k + \sqrt{v\varepsilon}} + C_{1\varepsilon}\frac{\varepsilon}{k} C_{3\varepsilon} C_b + S_\varepsilon \quad (9)$$

where the model constants are $C_{1\varepsilon}$= 1.44, C_2=1.9, σ_k=1.0, and σ_ε=1.2

The other governing conservation equation solved is the energy equation:

$$\partial\left(u_i(\rho\,\mathrm{E}\,+\,\mathrm{P})\right)/\partial \mathrm{x_j} = \nabla.\left[k_{eff}\nabla T\,-\,\sum_j h_i\,\vec{J_i}\,+\,\left(\bar{\tau}_{eff}.\bar{u}_i\right)\right]\,+\,S_h \tag{10}$$

where k_{eff} is the effective conductivity.

Steady Diffusion flamelet Model

The complexity of turbulence-chemistry interaction modeling can be avoided by using this model. In this non-premixed model, the thermochemistry can be reduced to one or two variable by using a certain assumption to convert the problem to a mixing problem. By using the mixture fraction approach, the combustion problem will include one or two conserved scalar transport equations and no need to solve separated equations for species concentrations. Instead, the species concentration can be found using equations derived from mixture fraction, ***f***.

The mixture fraction, f, is defined as the burnt and unburnt and fuel local element mass fraction. The flame is separated into a burnt and unburnt mixture of fuel and oxidizer. The value of f is one at the fuel jet and zero at the oxidizer jet.

The steady state conservation equation for the mixture fraction is:

$$\nabla.\left(\rho\,\overrightarrow{u_i}\,\bar{f}\right) = \nabla.\left(\left(\frac{k_m}{C_p}\,+\,\frac{\mu_t}{\sigma_t}\right)\nabla\,\bar{f}\right)\,+\,S_m\,+\,S_{user} \tag{11}$$

where k is the laminar thermal conductivity of the mixture, Cp is the specific heat of the mixture, and σ_t is the Prandtl number of a value 0.85. Also, S_{user} is the user-defined source term and Sm is the the source term that caused by the transfer of mass of liquid droplet or solid particules into the gas phase.

A final conversation is used for the mixture fraction variance in Ansys-Fluent:

$$\nabla.\left(\rho\,\overrightarrow{u_i}\,\overline{f'^2}\right) = \nabla.\left(\left(\frac{k_m}{C_p}\,+\,\frac{\mu_t}{\sigma_t}\right)\nabla\,\overline{f'^2}\right)\,+\,C_g\,\mu_t\,.\left(\nabla\,\bar{f}\right)^2 + C_d\,\rho\,\frac{\varepsilon}{k}\,\overline{f'^2} + \,S_{user} \tag{12}$$

where $f' = f\,-\,\bar{f}$, and Cg and Cd are constants of a values 2.86 and 2 respectively.

RESULT AND DISCUSSION

In this work, the bio syngas combustion in the air-assisted flare was analyzed using CFD to quantify performance of the new air-assisted flare operating at low syngas flowrates from the

DFBG. Three different flare gas flow rates (1, 2 and 3 ft/s) were consider in this study, with specific results shown in the following figures referred to by the letters a, b, and c respectively. The air assisted volumetric flow rate was held constant at 7.4 ft^3/s for all cases. The effect of low flare gas flow rates on the predicted CE is presented in the following sections.

Combustion efficiency

The combustion efficiency of the current design is shown in Figure 2. CE was calculated according to equation (1) and the values of all terms in that equations are extracted from CFD results. As shown in this figure the combustion efficiency is high because of the increase in the flowrate by using the current flare tip. This is due to that the increase in syngas flow will enhance the turbulence and mixing energy. All the three values of the CE have a value above 96.5. The flare performance with the CE of a value equal or above 96.5 is consider as a good performance flare.

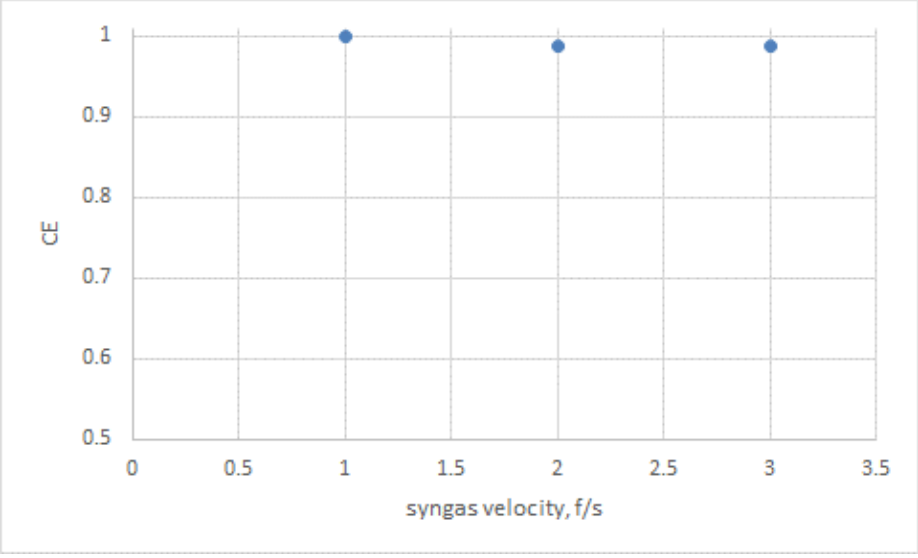

Figure 2 - Combustion efficiency for different inlet syngas velocities.

Temperature and Velocity counter.

The predicted gas temperature is shown on the vertical mid-plane of the computational domain for all cases in Figure 4. As shown, the average maximum temperature of the three cases is 1536°C, which compares well to the theoretical adiabatic flame temperature for a blend of H2 and CH4 (around 2000°C) and for CO (around 2100°F). When there is excess inert gases (CO_2, N_2) with high moisture content in syngas (~0.4), the flame temperature is reduced by quenched the flame by heating the inert gases and preheating the incoming unburnt fuel gas before they enter the combustion zone. Figure 3 shows the velocity contours for different inlet fuel flowrates. As shown, the flare tip velocity increased as the radial air flow increased. This is because the radial air acts as an aerodynamic nozzle to reduce the cross-sectional flow area in the flare which kept the tip velocity high and increased the mixing energy at the tip.

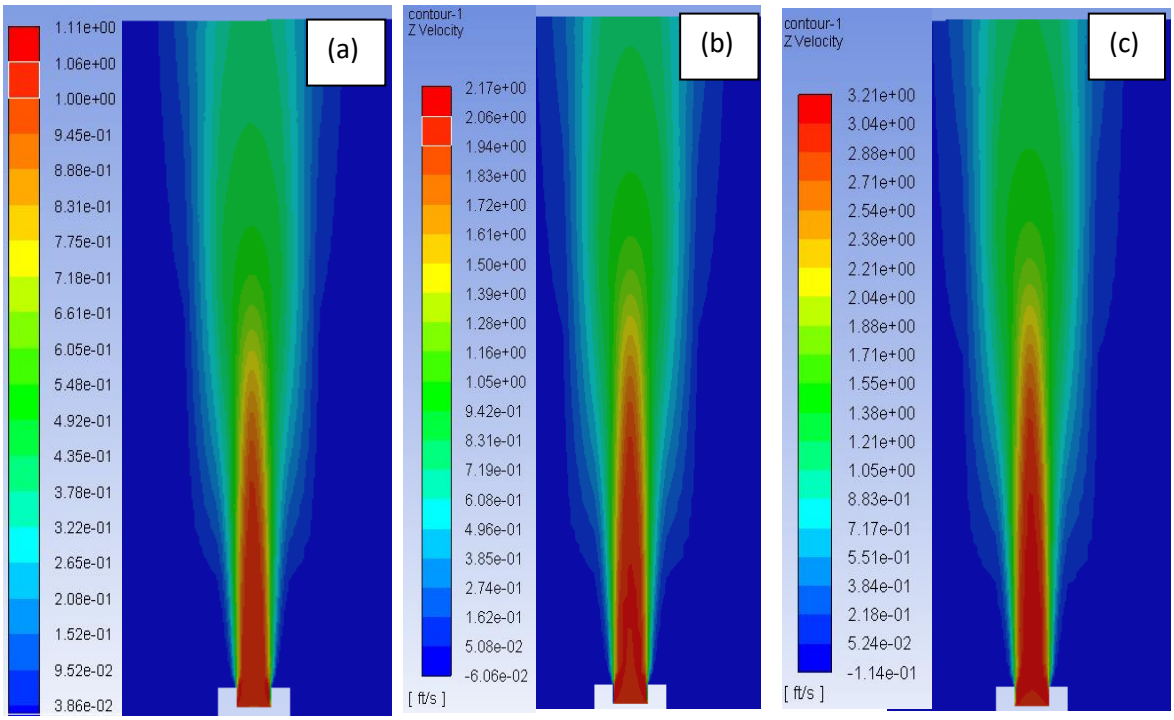

Figure 3 - Z-component velocity contour for different inlet syngas velocities.

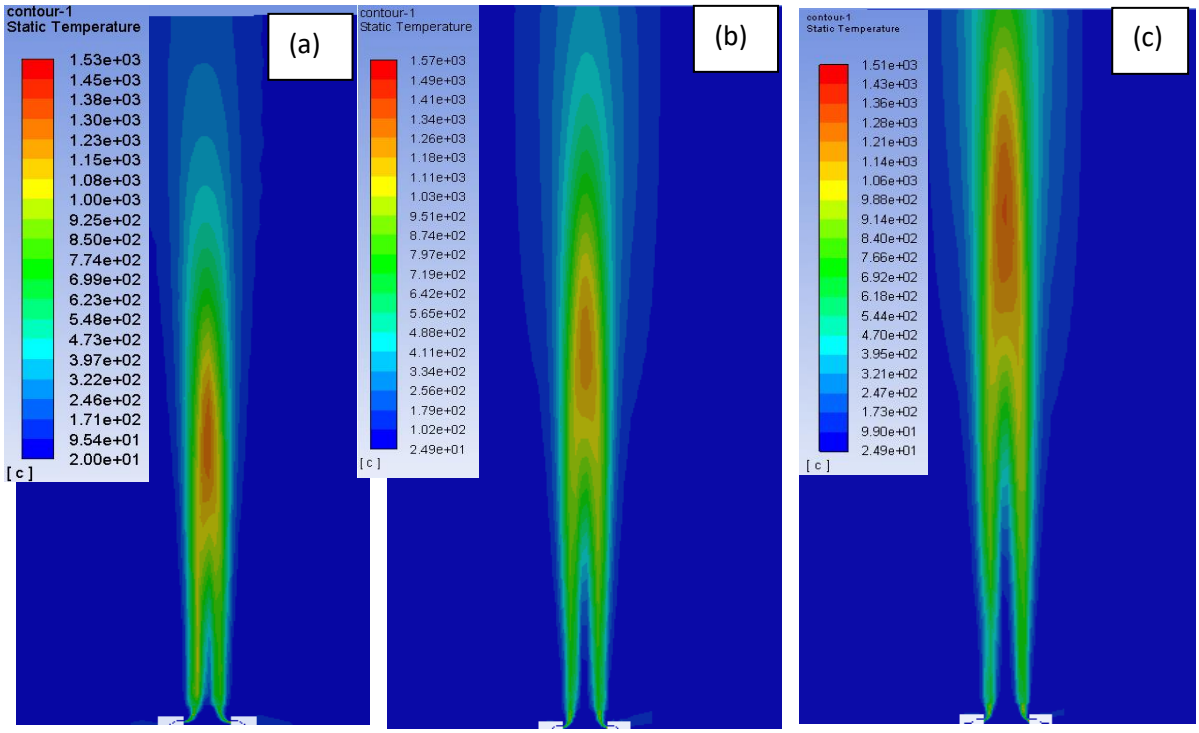

Figure 4 - Temperature contour for different inlet syngas velocities.

Mass Fraction

Figure 5, Figure 6, and Figure 7, present the counters of mass fractions of CO, CH_4, and H_2. As shown, the CO mole fraction decreased significantly ~20 in above the injection point for syngas velocity of 1 ft/s. For higher syngas feedrates, the reaction zone expanded with the CO reaction zone extending to ~42 in and ~ 51 in above the injection point for syngas velocities of 2 and 3 ft/s respectively.

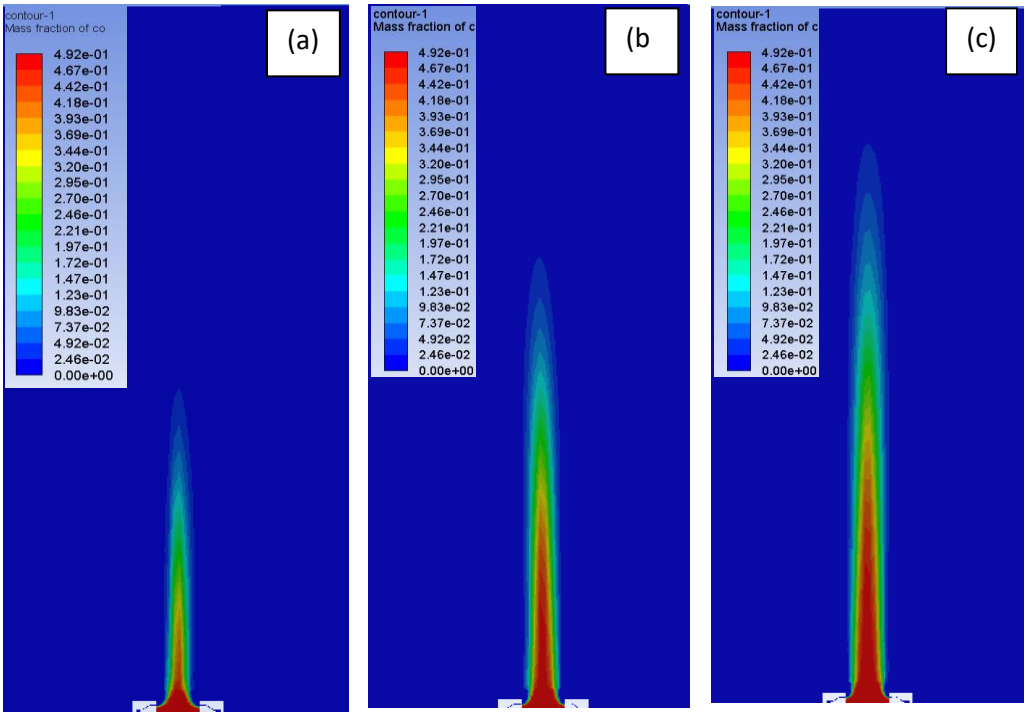

Figure 5 - Mass Fraction for CO for different inlet syngas velocities.

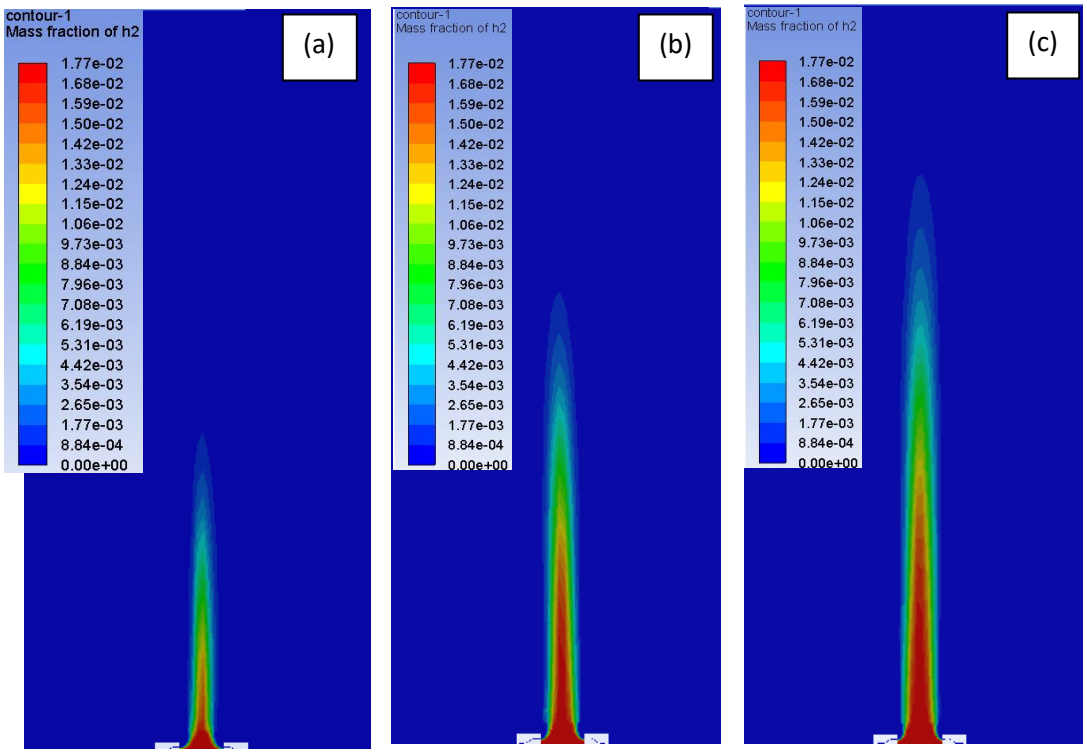

Figure 6 - Mass Fraction for CH4 for different inlet syngas velocities

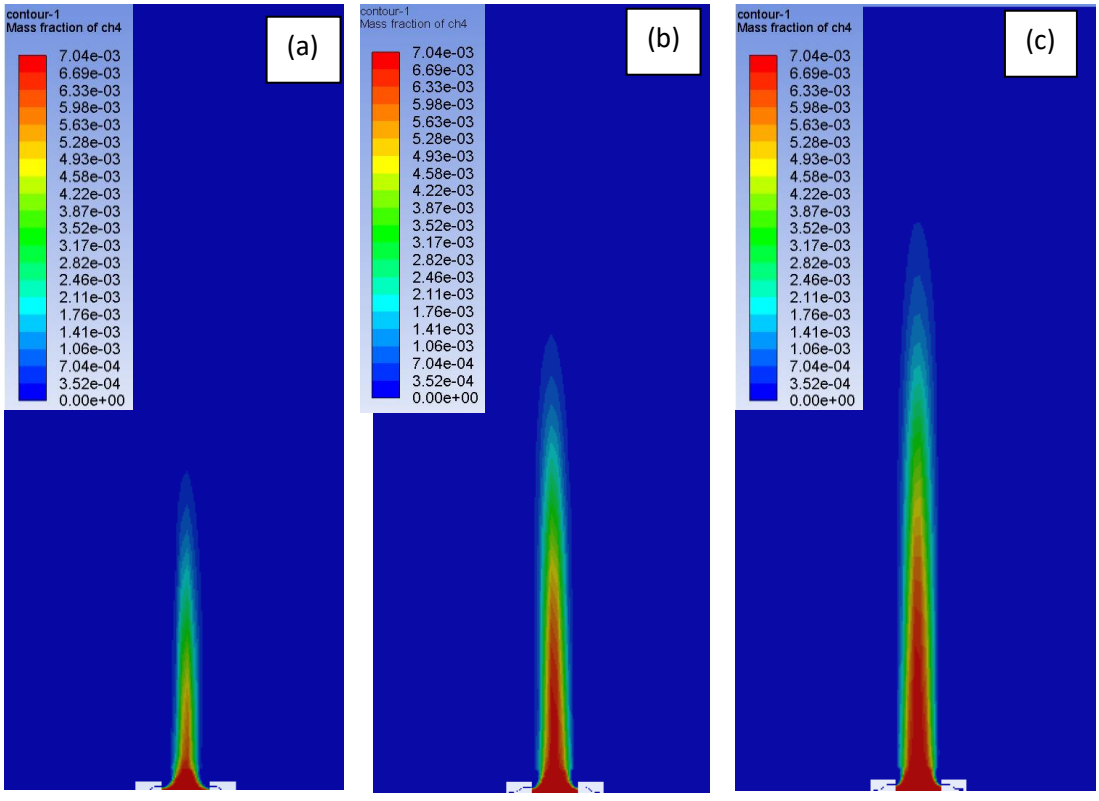

Figure 7 - Mass fraction of H2 for different inlet syngas velocities.

CONCLUSION

The combustion process in a new air assisted flare for burning bio syngas has been analyzed using a reacting flow model. Computational fluid dynamics was used to investigate flare performance for low flow conditions using a 22-species mechanism to describe the reaction kinetics. The RNG turbulence model was used to analyze the turbulent mixing above the flare tip. A non-premixed steady diffusion flamelet combustion model was utilized. High combustion efficiency (>0.98) were predicted for the new air flare design with bio syngas as the flare gas.

REFERENCES

[1] W. C. Nadaleti, G. Przybyla, L. Ziolkowski and P. B. Filho, "Analysis of emissions and combustion of typical biofuels generated in the agroindustry sector of Rio Grande do Sul State e Brazil: Bio75, syngas and blends," *Journal of Cleaner Production,* vol. 2018, pp. 988-998, 2019.

[2] A. Demirbas, "Biofuels sources, biofuel policy, biofuel economy and global biofuel projections," *Energy Conversion and Management,* vol. 49, no. 8, pp. 2016-2116, 2008.

[3] S. Sadaka, "Gasification, Producer Gas," [Online]. Available: https://www.uaex.edu/publications/PDF/FSA-1051.pdf.

[4] A. Bhavanam and R. C. Sastry , "Biomass Gasification Processes in Downdraft Fixed Bed Reactors: A Review," *International Journal of Chemical Engineering and Application,* vol. 2, no. 6, pp. 425-433, 2011.

[5] Quan Zhoua, C.S. Cheung, C.W. Leung Xiaotian Li, Xiaojie Li, Zuohua Huang, "Effects of fuel composition and initial pressure on laminar flame speed of H2/CO/CH4 bio-syngas," *Fuel,* vol. 238, pp. 149-158, 15 February 2019.

[6] K. Zhang and X. Jiang, "An investigation of fuel variability effect on bio-syngas combustion using uncertainty quantification," *Fuel,* vol. 220, pp. 283-295, 2018.

[7] D. T. V. Allen, "TCEQ flare study final report," TCEQ PGA No. 582-8-86245-FY09-04 and Task Order No. UTA10-000924-LOAT-RP9. Austin, TX: The University of Texas at Austin, The Center for Energy and Environmental Resources, 2011.

[8] Singh, K.D., Gangadharan, P., Chen, D.H., Lou, H.H., Li, X., Richmond, P., "Computational fluid dynamics modeling of laboratory flames and an industrial flare," *Journal of the Air and Waste Management Association,* vol. 64, no. 11, pp. 1328-1340, 2014.

[9] J. Smith, B. Adams, R. Jackson and A. Suo-Anttila, "Use of RANS vs LES Modelling for Industrial Gas-fired Combustion," *Industrial Combustion,* 2017.

[10] Vincent M. Torres, Scott Herndon, Zach Kodesh, and David T. Allen, "Industrial Flare Performance at Low Flow Conditions. 1. Study overview," *Industrial & Engineering Chemistry research,* vol. 51, pp. 12559-12568, 2012.

[11] Vincent M. Torres, Scott Herndon, and David T. Allen, "Industrial Flare Performance at Low Flow Conditions. 2. Steam- and Air-assisted Flare," *Industrial & Engineering Chemistry Research,* vol. 51, no. Vincent M. Torres, Scott Herndon, and David T. Allen, pp. 12569-12576, 2012.

[12] J. D. Smith, H. A. Al-Hameedi, R. Jackson and A. Suo-Antilla, "Testing and Prediction of Flare Emissions Created during Transient Flare Ignition," *Journal of Petrochemistry and Research,* vol. 2, no. 2, pp. 175-181, 2018.

[13] H. Golpour, "Design, Faabrication, operation and Aspen Simulation of oil shale pyrolysis and gasification process using moving bed downdraft reactor," Doctoral Dissertations. 2474, 2018. [Online]. Available: http://scholarsmine.mst.edu/doctoral_dissertations/2474.

[14] Hassan Golpour, Teja Boravelli, Joseph D. Smith, Hamid R. Safarpour, "Production of Syngas from Biomass Using a Downdraft Gasifier," *Int. Journal of Engineering Research and Application,* vol. 7, no. 6, pp. 61-71, 2017.

[15] J. Yu, "Experimental and numerical investigation on tar production and recycling in fixed bed biomass gasifier," Doctoral Dissertations, 2018. [Online]. Available: http://scholarsmine.mst.edu/doctoral/2693.

[16] J. Yu and J. D. Smith, "Validation and application of a kinetic model for biomass gasification simulation and optimization in updraft gasifiers," *Chemical Engineering and Processing - Process Intensification,* vol. 125, pp. 214-226, 2018.

[17] A. Abou-Taouk1, R. Sigfrid, R. Whiddon and L. E. Eriksson4, "A Four-Step Global Reaction Mechanism for CFD Simulations of Flexi-Fuel Burner for Gas Turbines," *Turbulence, Heat and Mass Transfer 7,* 2011.

[18] [Online]. Available: http://combustion.berkeley.edu/drm/drm22.dat.

[19] [Online]. Available: http://combustion.berkeley.edu/gri-mech/version30/text30.html.

[20] C. S. R. Baukal, The John Zink Combustion Handbook., New York, NY: CRC Press, 2001.

[21] Q. Zhou, C. Cheung, C. Leung, X. Li, X. Li and Z. Huang, "Effects of fuel composition and initial pressure on laminar flame speed of H2/CO/CH4 bio-syngas," *Fuel,* vol. 238, pp. 149-158, 2019.

[22] Tsan-Hsing Shih, William W. Liou, Aamir Shabbir, Zhigang Yang, Jiang Zhu, "A new k-ϵ eddy viscosity model for high reynolds number turbulent flows," *Computers & Fluids,* vol. 24, no. 3, pp. 227-238, March 1995.